Multiplexed high resolution soft x-ray RIXS

Y-D Chuang[1], C. Anderson[2], M. Benk[2], K. Goldberg[2], D. Voronov[1],

T. Warwick[1], V. Yashchuk[1] and H. A. Padmore[1*]

[1] Advanced Light Source, [2] Center for X-ray Optics
Lawrence Berkeley National Laboratory, 1 Cyclotron Road, Berkeley, CA 94720, USA

[*]Corresponding author: *hapadmore@lbl.gov*

Abstract. High-resolution Resonance Inelastic X-ray Scattering (RIXS) is a technique that allows us to probe the electronic excitations of complex materials with unprecedented precision. However, the RIXS process has a low cross section, compounded by the fact that the optical spectrometers used to analyze the scattered photons can only collect a small solid angle and overall have a small efficiency. Here we present a method to significantly increase the throughput of RIXS systems, by energy multiplexing, so that a complete RIXS map of scattered intensity versus photon energy in and photon energy out can be recorded simultaneously[1]. This parallel acquisition scheme should provide a gain in throughput of over 100.. A system based on this principle, QERLIN, is under construction at the Advanced Light Source (ALS).

Resonant Inelastic X-ray Scattering (RIXS) is a powerful photon in – photon out technique that allows study of the weak elementary excitations that determine the electronic behavior of complex electronic materials [2]. A wealth of information can be gathered on electron correlation and dynamics from such a measurement. A RIXS measurement requires that monochromatic light is incident on a sample, and the energy and momentum of the photons that are scattered are then analyzed. In addition, in a refinement of the technique, the polarization of the scattered photons is also analyzed. In a conventional experiment, RIXS spectra are recorded for selected energies around the elemental absorption edge, so that a RIXS map of scattered photon energy versus incident photon energy is built up sequentially. Although analysis of the scattered photons is a parallel process through use of a dispersive spectrograph, the measurement is still sequential, as the incident photon energy has to be incremented point by point through a core level resonance. Considering the width of the near edge region through which data is taken, and the ultimate energy resolution required, this ratio is typically several hundred. If a RIXS map were collected in parallel, then the overall acquisition could be sped up by this same factor. Here we describe a method for parallel acquisition of the RIXS map.

The idea of collecting a RIXS map in parallel was first proposed by Strocov [3]. In this original proposal, light was focused onto a sample from the dispersed exit plane of a monochromator by conventional K-B mirrors. The dispersed field (of height around 1 mm) contained all the energies that had to be imaged to a detector. This imaging was then performed with a second grazing incidence mirror in the spectrometer. In the orthogonal direction, scattered radiation from the line focus produced at the sample was dispersed and focused onto the detector. In this way, the detector plane had a mapping of the incoming and scattered photon energies in the vertical and horizontal directions respectively. The problem with this initial scheme was that the grazing incidence mirror used to project the exit plane of the monochromator onto the sample produces a focal plane that is tilted at a grazing angle. Only a vanishingly small height at the sample is in focus and this severely restricts the energy range that can be used, and makes the technique impractical. The same is true for the single mirror focusing from the sample to the detector. However, this obliquity of field, can be removed by correct use of two mirrors in a single imaging plane. This arrangement is widely used in x-ray astronomy for grazing incidence telescopes, such as Chandra (http://chandra.harvard.edu/index.html), where the flat object field at infinity has to be imaged to a flat image field on a detector. This arrangement was first described by Wolter [4]. In the original arrangement, the system was rotationally symmetric with a paraboloid followed by a hyperboloid in a confocal arrangement. In a system with an

Proceedings of the 12th International Conference on Synchrotron Radiation Instrumentation – SRI2015
AIP Conf. Proc. 1741, 050011-1–050011-5; doi: 10.1063/1.4952931
Published by AIP Publishing. 978-0-7354-1398-6/$30.00

object at finite distance and where we have separated imaging and dispersion as in our case, the system is modified to use elliptical and hyperbolic cylindrical mirrors.

Fig. 1 shows the arrangement of the monochromator to be used in this arrangement. A conventional varied line spacing (VLS) monochromator is followed by two elliptical mirrors. The function of these mirrors is to demagnify the large horizontal source size of the ALS storage ring to a 3 micron (FWHM) wide line at the sample and coincident with the monochromatic focal plane. This requires a demagnification of around 182:1. Due to the requirement to have a good working distance between the last mirror and the sample, this is carried out in two stages, with the first mirror having a demagnification of 78:1 and the second a demagnification of 2.3:1. This allows a 1.2 m distance between the center of the last elliptical mirror and the sample, safely placing this mirror outside the sample vacuum chamber. The intermediate focus formed by the first elliptical mirror also permits us to remove scatter with a pair of slits and is a convenient place to monitor and stabilize the beam position with a servo loop. The function of the VLS beamline monochromator is to produce a flat dispersed field perpendicular to the principal ray, over a field of around 2 mm. We therefore end up with a dispersed line 2 mm tall, by 3 microns (FWHM) wide, without use of the intermediate focus slits. The few micron narrow focus is the object for the following spectrograph, and therefore the width of the focus determines the spectral resolution. In order to obtain the required resolving power of 30,000, the width of the intermediate focus slit between the ellipses will be used to reduce the beam width at the focus to a hard edged 2 μm from its native 3 μm FWHM.

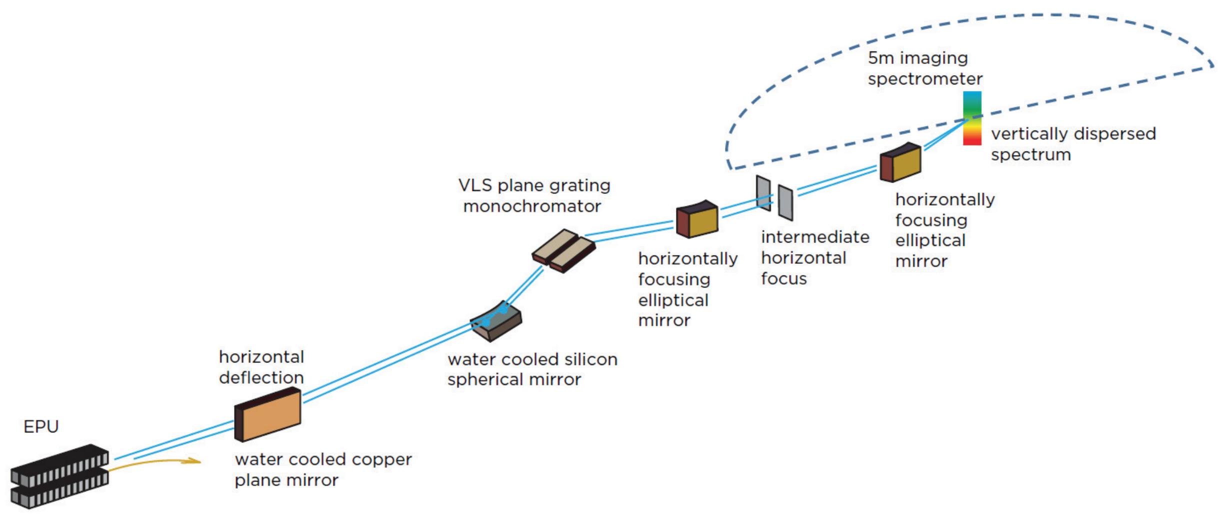

Figure 1. Optical layout of the Querlin beamline for multiplexed RIXS

The angular size of the non-dispersive horizontal focus is 1.7 μrads FWHM, resulting in a slope error specification of 0.18 μrads rms over the 600 mm length of the downstream elliptical mirror. Similar mirrors have been manufactured to significantly better tolerances using advances in fabrication and metrology methods[5] and have also been used in two stage demagnification schemes to reach a focus size below 50 nm[6].

The arrangement of the spectrometer is shown in Fig. 2 and is a standard Hettrick – Underwood varied line spacing (VLS) grating design, with the exception that the spherical mirror that produces a converging beam through the grating is replaced in this case by an elliptical mirror[7]. This mirror collects around 9 milliradians and use of an elliptical shape reduces the higher order correction terms that are needed in the polynomial representing the grating varied line spacing. Also a cylindrical rather than spherical shape is required as the latter would disturb imaging in the orthogonal direction. The system has an overall magnification of 10 at the center of the design energy range (700 eV) in order to match the monochromatic image size to the detector pixel size with adequate oversampling. The grating to be used is under development in our lab and we are pursuing a range of options as described below.

In the orthogonal direction we have used a modified Wolter imaging system. This maps the 2 mm tall dispersed input field from the monochromator onto the detector plane and thus requires a flat field imaging system. The system we chose for this project consists of a hyperbolic mirror to produce a virtual focus followed by an elliptical mirror to produce a real focus with a magnification of 5. Magnification is necessary due to the need to match the size of a wavelength resolution determining element for a resolving power of 30,000 on the sample to the pixel size of the detector with adequate oversampling. This also requires the use of a detector with a 5 μm pixel size.

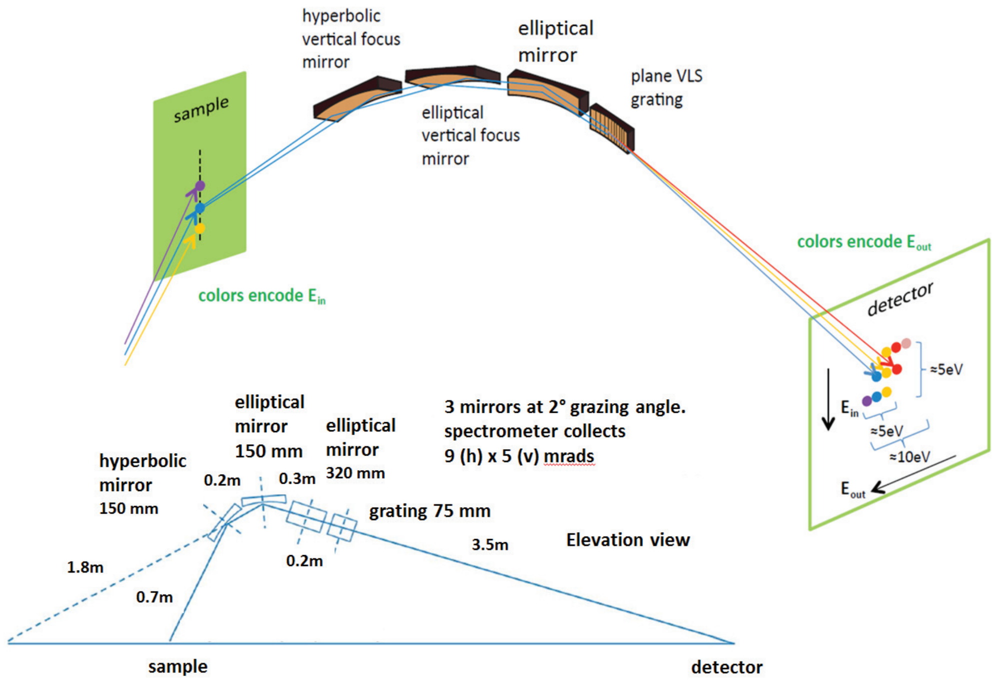

Figure 2. Diagram showing the concept of producing a RIXS map in a multiplexed geometry (upper) and dimensions of the system in the lower diagram

The hyperbola-ellipse configuration is one of many different arrangements that can be used. For example there are systems which involve concave – convex surfaces, convex – concave surfaces, each class with and without an intermediate focus and other variations. There are 8 general classes of Wolter optics, as outlined by Saha[8]. In addition there are freeform versions of each class in which polynomial surfaces are used. The design of these types of system is described by Chase et al[9].

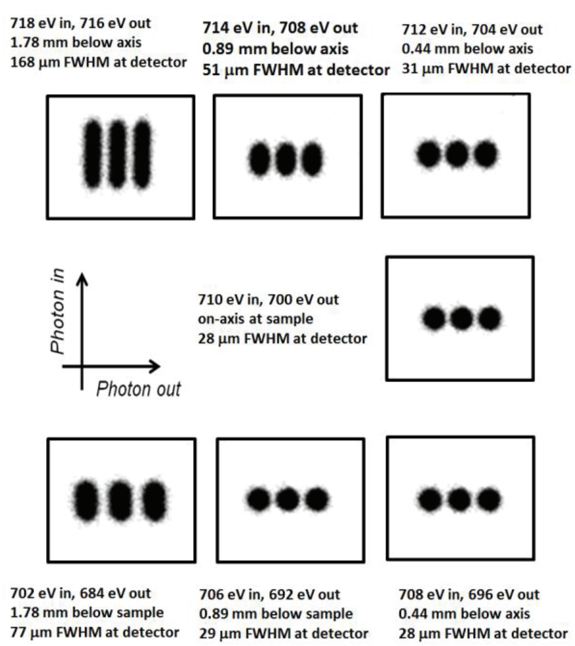

Figure 3. Dispersion and imaging characteristics of the multiplexed system[1]

All of these Wolter systems involve rotationally symmetric optics, compared to the 1d focusing required in our design. We evaluated the performance of some of these systems with the conclusion that in the case of 1d focusing and our range of field sizes, the off axis imaging of the modified classical type I system is as good as these other more complex designs. A simulation of the overall dispersion and imaging quality is shown in Fig. 3. The spectrometer resolution remains essentially unchanged over a large range of scattered energies (684 – 716 eV) as expected, given the nature of the flat field focusing in the Hettrick – Underwood VLS design. In the incident photon energy direction (vertical in the figure and physically in the design), the image is essentially aberration free for the resolving power required, from 706 to 712 eV. This represents ~ 250 energy channels at the design resolving power and this is the effective gain in throughput compared to a normal monochromatic input RIXS system. It can be seen in Fig. 3 that the performance outside this range starts to rapidly deteriorate. This is due to the main aberration in a Wolter system, that of field curvature. The imaged field is perpendicular on axis with respect to the principal ray, but it is curved . This results in a defocus error that grows as the square of the off-axis coordinate position.

The final optical component required is the grating. Due to the high resolving power required and the limited space available, a grating with a high line density is needed. Unfortunately high line density gratings have a low diffraction efficiency due to shadowing, typically < 5%. A way around this problem is to use blazed multilayer gratings (MLG) in above 1^{st} order[10, 11]. Below we show one of the candidate gratings that we have fabricated. For the central design energy of 700 eV, the efficiency in 2^{nd} order of a 2500 l/mm grating is 14% as shown in Fig. 4 with a groove efficiency of 64%. With an optimized MLG, an efficiency above 20% should be achievable.

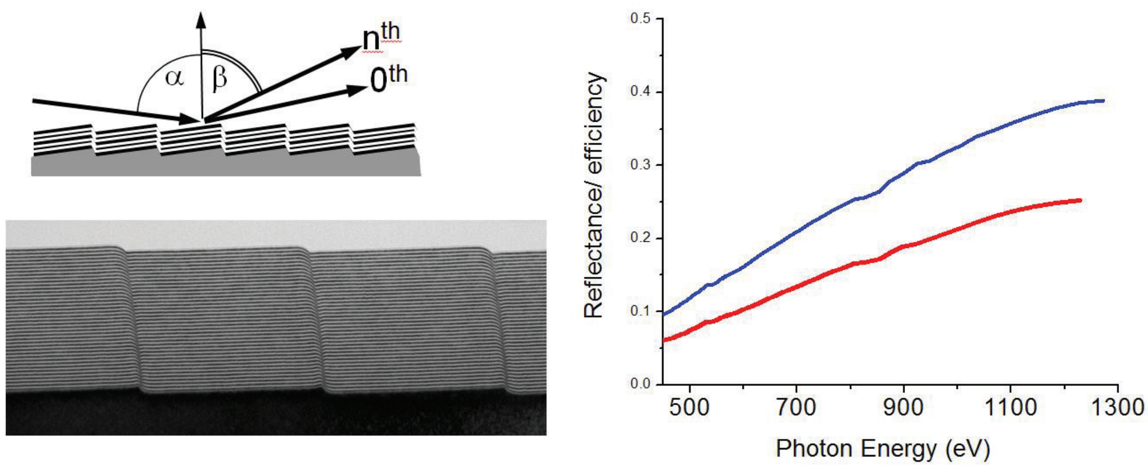

Fig. 4 Performance of a 2^{nd} order 2500 l/mm blazed multilayer grating. In the right hand diagram, the reflectivity of a multilayer witness sample is shown (blue) against the absolute efficiency of the grating.

In summary, we are constructing a new system that will enable RIXS to be carried out in a multiplexed fashion, so that a full RIXS map is recorded in parallel. This involves several technologies that are new in the RIXS field, the use of Wolter imaging optics, small pixel CMOS detectors, and multilayer gratings.

The work was supported by the US Department of Energy under contract number DE-AC02-05CH11231.

REFERENCES

1. [1]T. Warwick, Y.-D. Chuang, D. Voronov and H. A. Padmore Journal of Synchrotron Radiation**,** (2014).
2. [2]L. J. P. Ament, M. van Veenendaal, T. P. Devereaux, J. P. Hill and J. van den Brink Reviews of Modern Physics **83,** (2011).
3. [3]V. N. Strocov Journal of Synchrotron Radiation **17,** (2010).
4. [4]H. Wolter Annalen der Physik **445,** (1952).
5. [5]K. Yamamura, K. Yamauchi, H. Mimura, Y. Sano, A. Saito, K. Endo, A. Souvorov, M. Yabashi, K. Tamasaku, T. Ishikawa and Y. Mori Review of Scientific Instruments **74,** (2003).
6. [6]H. Mimura, H. Yumoto, S. Matsuyama, T. Koyama, K. Tono, Y. Inubushi, T. Togashi, T. Sato, J. Kim, R. Fukui, Y. Sano, M. Yabashi, H. Ohashi, T. Ishikawa and K. Yamauchi Nat Commun **5,** (2014).

7. [7]M. C. Hettrick, J. H. Underwood, P. J. Batson and M. J. Eckart Applied Optics **27,** (1988).
8. [8]T. T. Saha Applied Optics **26,** (1987).
9. [9]R. C. Chase and L. P. VanSpeybroeck Applied Optics **12,** (1973).
10. [10]D. L. Voronov, L. I. Goray, T. Warwick, V. V. Yashchuk and H. A. Padmore Opt. Express **23,** (2015).
11. [11]D. L. Voronov, E. M. Gullikson, F. Salmassi, T. Warwick and H. A. Padmore Optics Letters **39,** (2014).